Hydrogen gas formation from the Photolysis of Rhenium Hydrides – Mechanistic and Computational studies

Alyssa A. Webster,[a] Jianqiang Huo,[a] Jenna Milliken,[a] Pat Sullivan,[a,c] Jan Kubelka,[b,*] and John O. Hoberg [a,*]

[a] Department of Chemistry, University of Wyoming

[b] Department of Petroleum Engineering, University of Wyoming

Table of Contents

1. General Information

All reagents were ACS grade and were used without further purification. All reactions were conducted in a dried apparatus under an argon atmosphere unless otherwise stated. Solvents were dried and purified before use. Reaction progress was monitored using pre-coated TLC plates with silica UV^{2}54 and visualized by UV radiation (λ = 254 nm). ^{1}H spectra were recorded with deuterated solvents using a Bruker Avance 400 MHz NMR spectrometer, calibrated using residual protonated solvent as an internal reference (^{1}H, residual $CHCl_3$). Chemical shifts (δ) are reported in parts per million (ppm) and coupling constants (J) are measured in hertz (Hz). The following abbreviations are used to describe multiplicities: s = singlet, d = doublet, t = triplet, q = quartet, br = broad, m = multiplet. Fourier-transform infrared (FT-IR) spectroscopy was performed with a Perkin Elmer Spectrum One spectrometer using freshly prepared potassium bromide pellets and recorded in the range of 450-4000 cm^{-1} and averaged over twelve scans with background subtraction. Absorption bands were measured in wavenumbers (cm^{-1}), and only peaks of interest were reported. Absorption spectroscopy (UV-Vis) was obtained with an Agilent 8453 UV-Visible spectrophotometer over the range 220-1100 nm using a quartz cuvette with 1 cm path length referenced against a solvent blank. All samples were dissolved in acetonitrile ,and spectra were acquired at 20 °C in air. Mass spectra (m/z) and HRMS were recorded on a Voyager-DE PRO MALDI-TOF mass spectrometer. Rhenium chloride complexes $[Re(4,4'\text{-}R_2\text{-bpy})(CO)_3Cl]$ were synthesized as previously reported.[1] Rhenium tricarbonyl hydrides **1a** – **1d** were synthesized as previously reported.[2,3] ^{1}H NMR data for **1c** and **1d,** which are not reported, are provided below. For convenience, the general synthesis for all rhenium triflate and hydrides is given for **1e**.

2. Preparation of the Rhenium Hydride Complexes

4,4'-dimethoxy-2,2'-bipyridine rhenium tricarbonyl triflate.

^{1}H NMR $CDCl_3$: δ 8.64 (d, J = 6.3 Hz, 2H), 8.17 (d, J = 2.6 Hz, 2H), 7.07 (dd, J = 6.4, 2.6 Hz, 2H), 4.21 (s, 6H) ppm. IR (neat): 2030, 1907, 1255, 1032 cm^{-1}.

4,4'-dimethoxy-2,2'-bipyridine rhenium tricarbonyl hydride (1c).

^{1}H NMR d^6-Acetone: δ 8.95 (d, J = 6.4 Hz, 2H), 8.16 (d, J = 2.7 Hz, 2H), 7.26 (dd, J = 6.4, 2.6 Hz, 2H), 4.12 (s, 6H), 2.00 (s, 1H) ppm. IR (KBr): 1999, 1881, 1854 cm^{-1}. UV-VIS (MeCN): $\lambda_{max, abs}$: 356 nm. Fluorescence (MeCN) $\lambda_{max, em}$: 550 nm.

4,4'-dichloro-2,2'-bipyridine rhenium tricarbonyl triflate

^{1}H NMR $CDCl_3$: δ 9.31 (d, J = 5.36 Hz, 2H), 8.48 (s, 2H), 7.86 (d, J = 5.64 Hz, 2H) ppm. IR (neat): 2033, 1905, 1250, 1030 cm^{-1}.

4,4'-dichloro-2,2'-bipyridine rhenium tricarbonyl hydride (1d).

^{1}H NMR d^6-Acetone: δ 9.28 (d, J = 6.1 Hz, 2H), 8.86 (d, J = 2.1 Hz, 2H), 7.79 (dd, J = 6.0, 2.1 Hz, 2H), 1.70 (s, 1H) ppm. IR (KBr): 2005, 1900, 1876 cm^{-1}. UV-VIS (MeCN): $\lambda_{max, abs}$: 396 nm. Fluorescence (MeCN) $\lambda_{max, em}$: 567 nm.

4,4'-dibromo-2,2'-bipyridine rhenium tricarbonyl triflate

A 25 ml flask was loaded with 4,4'-dibromo-2,2'-bipyridine rhenium tricarbonyl chloride (125 mg, 0.202 mmol), silver triflate (54 mg, 0.212 mmol), and CH_2Cl_2 (8 ml). The solution was stirred at r.t. overnight in darkness. The orange solution was vacuum filtered through diatomaceous earth, washed with methylene chloride, and concentrated to a solid. The orange solid was purified through recrystallization with CH_2Cl_2/Et_2O at 0 °C to yield an orange solid (106 mg, 72%). ^{1}H NMR $CDCl_3$: δ 9.52 (d, J = 5.8 Hz, 2H), 8.55 (s, 2H), 7.95 (d, J = 5.8 Hz, 2H) ppm. IR (KBr): 2029, 1922, 1888, 1233, 1008 cm^{-1}.

4,4'-dibromo-2,2'-bipyridine rhenium tricarbonyl hydride (1e).

A 25 ml flask was loaded with 4,4'-dibromo-2,2'-bipyridine rhenium tricarbonyl triflate (106 mg, 0.145 mmol), MeOH (6 ml), and cooled to 0 °C. $NaBH_4$ (109 mg, 2.897 mmol) was added, and the solution was stirred for 1 h at 0 °C. The solution was warmed to r.t. and continued to stir for 1.5 h. The resulting solution was vacuum filtered and the dark orange precipitate was washed with water (20 ml) and dried under reduced pressure to yield a dark orange precipitate (62 mg, 74%) ^{1}H NMR d^6-Acetone: δ 9.11 (d, J = 6.00 Hz, 2H), 9.00 (s, 2H), 7.92 (d, J = 6.00 Hz, 2H), 1.68 (s, 1H) ppm. IR (KBr): 2025, 1999, 1878 cm^{-1}. UV-VIS (MeCN): $\lambda_{max, abs}$: 407 nm. Fluorescence (MeCN) $\lambda_{max, em}$: 568 nm.

2,2'-BipyridineRhenium Tricarbonyl Deuteride

A solution of 2,2'-bipyridine rhenium tricarbonyl triflate (30 mg, 0.07 mmol) in CD_3OD(2 mL) was heated to reflux and $NaBD_4$ (29 mg, 0.7 mmol) was slowly added. After 2 h at reflux, the reaction was cooled to room temperature and 1 mL of D_2O was added. The resulting solution was filtered and the red precipitate was washed with D_2O (2mL) and dried under reduced pressure to afford an orange solid (10 mg, 42%, Deuterium incorporation was calculated to be >85% based on ^{1}H NMR comparison of Bpy resonances). ^{1}H NMR (Acetone-d6): δ 9.24(d, *J*=5.2Hz, 2H), 8.65 (d, *J*=8.1Hz, 2H), 8.23 (t, *J*=7.6Hz, 2H), 7.67(t, *J*=5.7Hz, 2H). IR (neat): 1998, 1901, 1885cm-1.

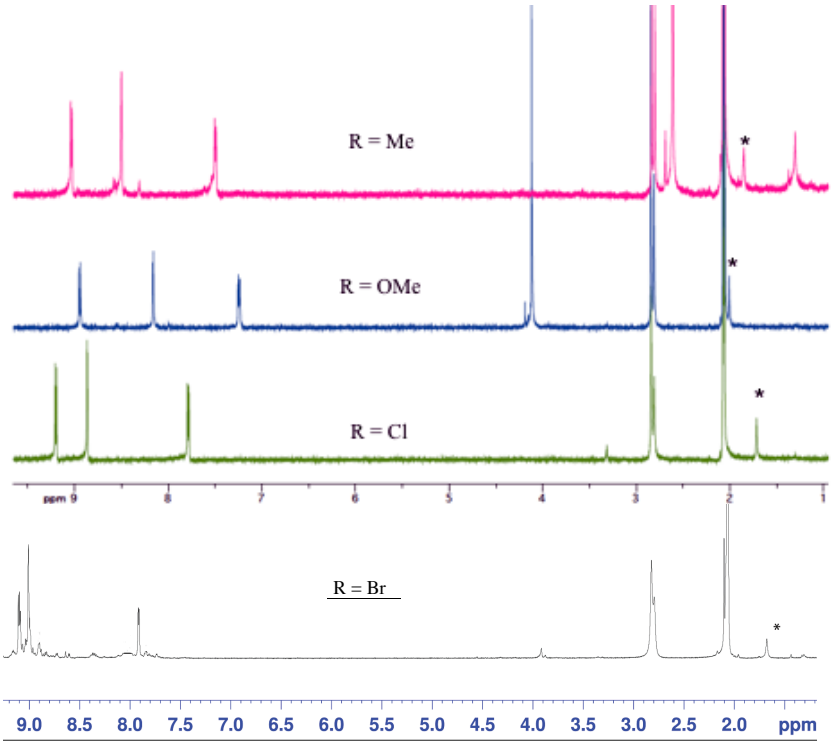

Figure S1. ^{1}H NMR comparison of complexes **1b, 1c, 1d** and **1e**, * denotes the Re-H signal. Sample **1e** (R = Br), bottom spectrum, was obtained 1-2 yrs post synthesis and noticeable decomposition occurred. Residual water peak in all spectra occurs at 2.8 ppm.

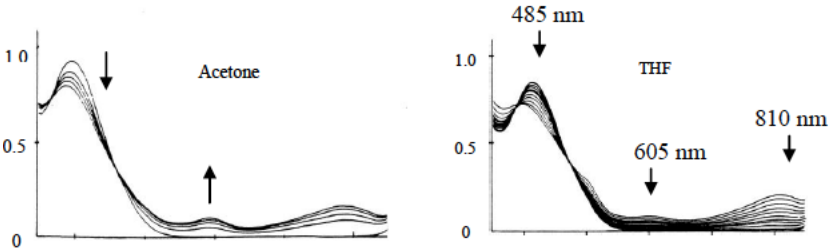

Figure S2. UV-Vis absorption study of the photolysis in acetone and THF showing the disappearance of the Re-H at 485 nm and appearance of the dimer at 605 and 810nm.

Computational Methods:

All computations were carried out using Gaussian 09 quantum chemistry package.[4] Optimizations of model structures and subsequent vibrational calculations were done at density functional theory (DFT) level using B3LYP functional with the following basis set: 6-31+G(d) for N and O, 6-31G(d) for C and H and LANL2DZ for Re. The basis set is similar to that used in previous studies of $[Re(bpy)CO_3]_2$ complexes,[5] but it is larger and more balanced by inclusion of polarization functions as well as diffuse functions on O and N. Further, to correct for the deficiency of the DFT methods in accounting for dispersion forces, Grimme empirical dispersion correction[6] (GD3) was included. The solvent environment – acetone and tetrahydrofuran (THF) - was approximated in optimizations, frequency and excited state calculations by the conductor-like polarized continuum model (CPCM). In addition, the energies were computed for the optimized structures with the SMD implicit solvent model, which also accounts for the cavity and dispersion contribution to solvation.[7] Since there is no rigorous or universally agreed upon optimal way to evaluating thermodynamic parameters for condensed phase systems, three different ways[8] were used to compute the Gibbs free energies of the model structures in acetone or THF solutions and compared. The first is based on electronic, zero-point (ZPE) and thermal energies all computed with the CPCM, the second combines the electronic energy calculated using SMD model with the ZPE and thermal contributions obtained from CPCM calculations[8] and third again combines SMD electronic energy with CPCM calculations but includes only ZPE and vibrational thermal energy only (i.e. translational and rotational contributions are neglected).

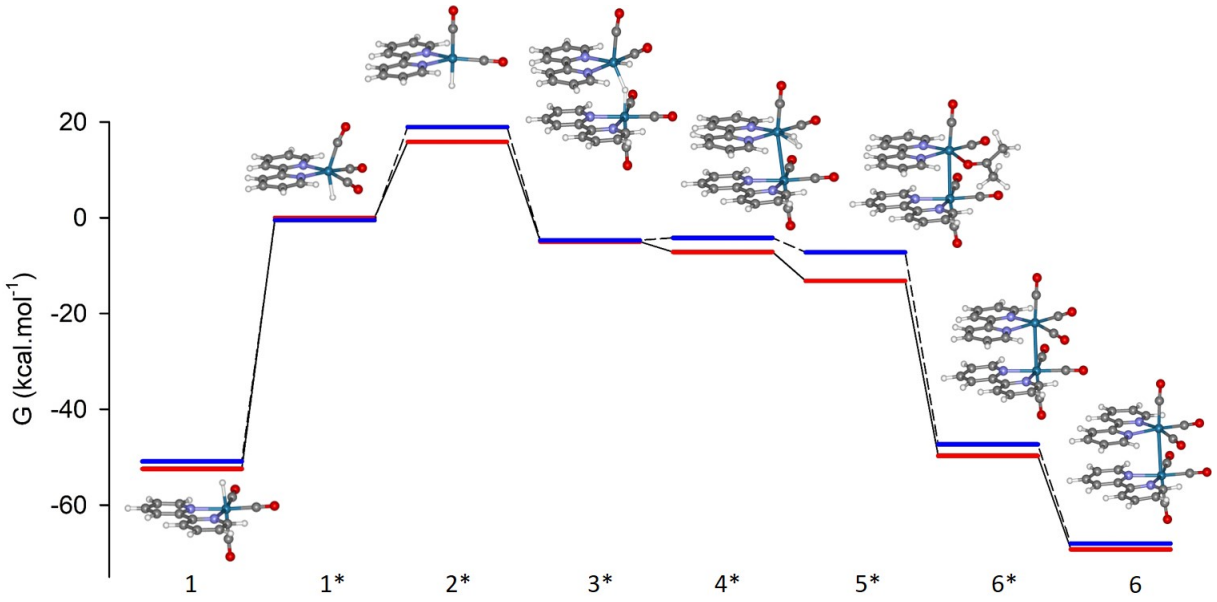

Figure S3. Schematic energy diagram for the proposed reaction mechanism. Gibbs free energy calculated using corrected SMD method (see text for details) is plotted for each of the chemical species relative to the reactant species: **1** (singlet ground state $Re(bpy)(CO_2)_3H$), **1*** (triplet excited state $Re(bpy)(CO_2)_3H$) and solvent (acetone or THF). The red levels correspond to the reaction in acetone, the blue levels in THF. The numbering follows that in Scheme 2 (see also Figure 4).

Table S1: Geometric parameters of #1 ($Re(bpy)(CO_2)_3H$) in the ground (singlet) state, excited (triplet) state, 2* ($Re(bpy)(CO_2)_2H$) in excited (triplet) state (C_s symmetry)[a] and 2 in the ground (singlet) state.

property/species	1	1*	2*	2
Bond length (Å)				
Re–N	2.206	2.142	2.193	2.186
Re–C (equatorial CO)	1.915	1.953	1.946	1.889
Re–C (axial CO)	1.964	1.979	1.926	1.933
Re–H	1.756	1.742	1.780	1.786
C–O (equatorial CO)	1.171	1.158	1.176	1.184
C–O (axial CO)	1.767	1.161	1.180	1.179
Bond angle (deg)				
Re–C–O (axial CO)	178.5	171.2	178.8	176.5

Re–C–O (equatorial CO)	177.9	177.2	179.3	177.3
N–Re–N	74.1	76.9	73.4	76.4
N–Re–C (equatorial COs)	169.8/97.6	167.1/93.3	142.9	171.7/96.4
N–Re–C (axial CO)	93.0	104.2	93.2	93.0
N–Re–H	83.8	96.3	86.1	85.4
C–Re–C (equatorial COs)	93.3	95.0	-	
C–Re–H (axial CO)	175.9	153.8	179.8	171.3

[a]Structures optimized at B3LYP/6-31(d)(C,H)/6-31+G(d)(N,O)/LANL2DZ(Re) with CPCM implicit solvent model for acetone.

Table S2: Geometric parameters of the reaction intermediates 3*, 4*, 5* and products 6* and 6[a]

property/species	3*	4*	5*	6*	6
Bond length (Å)					
Re–Re	3.363	3.253	3.277	3.264	3.190
Re–N(1)[b]	2.186/2.194	2.171/2.159	2.162/1.181	2.166	2.167
Re–N(2)[b]	2.179/2.159	2.169/2.098	2.165/2.108	2.166	2.173
Re–C(1) (equatorial CO)[b]	1.926/1.901	1.924/1.910	1.926/1.884	1.927	1.922
Re–C(2) (equatorial CO)	1.925	1.927	1.927	1.931	1.921
Re–H (bridging H)[b]	1.896/1.781	-	-	-	-
Re–H (bound H/H_2)	1.706	1.824/1.818[c]	-	-	-
Re–O (solvent)	-	-	2.133	-	-
Re–C (axial CO)[b]	1.917/1.924	1.886/1.870	1.884/1.851	1.885	1.900
Bond angle (deg)					
Re–Re–N(1)[b]	79.3/93.0	84.6/93.3	89.9/90.5	89.6	88.0
Re–Re–N(2)[b]	89.5/99.6	84.2/89.9	84.8/85.5	85.1	88.8
Re–Re–C(1) (equatorial CO)[b]	98.2/85.6	87.9/83.5	84.9/81.8	87.0	84.6
Re–Re–C(2) (equatorial CO)	83.5	83.5	86.6	86.2	83.4
Re–H–Re (bridging H)	132.3	-	-	-	-
Re–Re–H (bound H/H_2)	92.3	70.2/95.0	-	-	-
Re–Re–O (solvent)	-	-	83.8	-	-
Re–Re–C (axial CO)[b]	168.4/162.1	178.8/168.3	173.2/172.6	175.8	175.3
Re–C(1)–O (equatorial CO)[b]	178.9/178.6	177.8/177.9	177.7/177.4	178.6	178.1
Re–C(2)–O (equatorial CO)	177.4	179.1	178.2	178.7	178.2
Re–C–O (axial CO)[b]	179.1/175.2	179.6/178.2	178.9/178.2	179.6	176.9
N–Re–N[b]	75.3/75.1	75.3/76.6	75.4/76.3	75.4	74.6
C–Re–C (equatorial COs)	90.5	90.2	90.7	89.8	90.4
C(1)–Re–H (eq. CO, bridging H)[b]	81.9/91.2	-	-	-	-
C(2)–Re–H (eq. CO, bridging H)	99.8	-	-	-	-
C–Re–H (eq. CO, bound H/H_2)	97.9	84.1/98.2	-	-	-
C–Re–O (eq. CO, solvent)	-	-	98.8	-	-
Dihedral angle (deg)					
N(1)–Re–Re–N(1)	46.4	39.9	39.2	35.3	24.9
C(1)–Re–Re–C(1) (equatorial COs)	62.2	51.7	53.09	49.3	41.8
C(1)–Re–Re–H (eq. CO, bound H/H_2)	-40.6	-34.4/-46.1[c]	-	-	-
C(1)–Re–Re–O (eq. CO, solvent)	-	-	-46.4	-	-
C–Re–Re–C (axial COs)	-156.4	-85.5	33.9	-17.9	-75.0
Re–Re–C–O (axial CO)[b]	-159.1/-1.6	27.0/89.9	-19.0/74.9	-5.5	6.6

[a]Structures optimized at B3LYP/6-31(d)(C,H)/6-31+G(d)(N,O)/LANL2DZ(Re) with CPCM implicit solvent model for acetone. Numbering corresponds to Figure 4. Product complexes 6 and 6* have C_2 symmetry (skew-cis arrangements, Fig. XX).

[b]In complexes 3*, 4* and 5* the first value corresponds to Re bound to 3 CO groups, second to the CO and H (complex 3*), CO and H^2 (complex 4*), or CO and solvent (complex 5*)

[c]The first value is for Re(2)-H(1), the second for Re(2)–H(2) in Figure 4. H-H distance is 0.860

Table S3: Geometric parameters of the reaction intermediates 3, 4, 5. (singlet states).

property/species	3	4	5
Bond length (Å)			
Re–Re	3.475	3.182	3.196
Re–N(1)[b]	2.207/2.203	2.174/2.167	2.161/2.157
Re–N(2)[b]	2.220/2.197	2.159/2.106	2.170/2.106
Re–C(1) (equatorial CO)[b]	1.921/1.923	1.924/1.922	1.921/1.923
Re–C(2) (equatorial CO)	1.880	1.901	1.885
Re–H (bridging H)[b]	1.837/1.780	-	-
Re–H (bound H/H_2)	1.715	1.796/1.812[c]	-
Re–O (solvent)	-	-	2.153
Re–C (axial CO)[b]	1.941/1.884	1.894/1.903	1.900/1.870
Bond angle (deg)			
Re–Re–N(1)[b]	79.3/93.0	88.1/88.3	88.5/88.6
Re–Re–N(2)[b]	90.2/85.3	87.8/90.8	89.5/87.2
Re–Re–C(1) (equatorial CO)[b]	81.2/87.0	86.2/81.6	82.5/81.4
Re–Re–C(2) (equatorial CO)	84.7	86.0	86.2
Re–H–Re (bridging H)	147.8	-	-
Re–Re–H (bound H/H_2)	88.6	65.2/93.3	-
Re–Re–O (solvent)	-	-	83.7
Re–Re–C (axial CO)[b]	173.7/175.0	174.9/171.7	174.8/173.3
Re–C(1)–O (equatorial CO)[b]	178.3/178.4	178.0 /177.9	176.5/178.0
Re–C(2)–O (equatorial CO)	177.4	177.4	176.3
Re–C–O (axial CO)[b]	178.2/179.5	177.7/176.8	176.6/177.3
N–Re–N[b]	77.4/73.7	74.5/75.9	74.5/75.9
C–Re–C (equatorial COs)	89.6	90.6	91.1
C(1)–Re–H (eq. CO, bridging H)[b]	97.4/91.2	-	-
C(2)–Re–H (eq. CO, bridging H)	97.8	-	-
C–Re–H (eq. CO, bound H/H_2)	94.9	88.7/95.9	-
C–Re–O (eq. CO, solvent)	-	-	99.4
Dihedral angle (deg)			
N(1)–Re–Re–N(1)	45.8	24.8	26.5
C(1)–Re–Re–C(1) (equatorial COs)	48.3	39.9	43.8
C(1)–Re–Re–H (eq. CO, bound H/H_2)	-53.3	90.4/92.9[c]	-
C(1)–Re–Re–O (eq. CO, solvent)	-	-	-56.2
C–Re–Re–C (axial COs)	-66.7	-98.9	-40.9
Re–Re–C–O (axial CO)[b]	-78.4/168.5	16.0/166.3	-9.3/89.1

[a]Structures optimized at B3LYP/6-31(d)(C,H)/6-31+G(d)(N,O)/LANL2DZ(Re) with CPCM implicit solvent model for acetone. Numbering corresponds to Figure 4. Product complexes 6 and 6* have C_2 symmetry (skew-cis arrangements, Fig. 3).

[b]In complexes 3*, 4* and 5* the first value corresponds to Re bound to 3 CO groups, second to the CO and H (complex 3*), CO and H^2 (complex 4*), or CO and solvent (complex 5*)

[c]The first value is for Re(2)-H(1), the second for Re(2)–H(2) in Figure 4. H-H distance is 0.889

Table S4: Energies and free energies at 298K in kcal.mol^{-1} of the reaction intermediates relative to the reactant species: 1 (singlet ground state Re(bpy)(CO$_2$)$_3$H), 1* (triplet excited state Re(bpy)(CO$_2$)$_3$H) and solvent (acetone or THF)[a]

Acetone					
	ΔE (SMD)[b]	**ΔE (CPCM)[c]**	**ΔG (CPCM)[c]**	**ΔG (SMD corr.)[d]**	**ΔG (SMD vib. only)[e]**
#1 (singlet)	-56.0	-55.5	-51.9	-52.4	-53.5
#2 (singlet)	-2.4	2.6	-5.5	-10.5	0.8
#2* (triplet)	26.8	29.7	18.8	15.9	27.9
#3 (singlet)	-42.6	-44.3	-35.7	-34.0	-42.3
#3* (triplet)	-11.0	-12.0	-6.0	-5.0	-12.6
#4 (singlet)	-33.2	-34.3	-24.3	-23.3	-31.6
#4* (triplet)	-14.7	-15.5	-8.0	-7.1	-14.8
#5 (singlet)	-39.5	-43.8	-29.0	-24.7	-41.8
#5* (triplet)	-24.0	-28.5	-17.7	-13.2	-29.7
#6 (singlet)	-82.4	-81.1	-67.9	-69.3	-82.7
#6* (triplet)	-59.8	-58.5	-48.4	-49.7	-62.5
THF					
	ΔE (SMD)[b]	**ΔE (CPCM)[c]**	**ΔG (CPCM)[c]**	**ΔG (SMD corr.)[d]**	**ΔG (SMD vib. only)[e]**
#1 (singlet)	-54.6	-54.3	-50.6	-50.8	-51.5
#2 (singlet)	1.9	4.59	-5.4	-8.0	5.3
#2* (triplet)	30.0	31.2	20.2	19.0	31.5
#3 (singlet)	-39.2	-42.1	-34.3	-31.4	-39.2
#3* (triplet)	30.0	31.2	20.2	19.0	31.5
#4 (singlet)	-31.1	-33.4	-24.0	-21.7	-29.5
#4* (triplet)	-10.1	-12.0	-6.6	-4.7	-11.9
#5 (singlet)	-35.6	-40.0	-25.6	-21.2	-38.3
#5* (triplet)	-18.6	-23.8	-12.4	-7.2	-23.6
#6 (singlet)	-80.7	-80.3	-67.7	-68.0	-81.1
#6* (triplet)	-56.9	-57.7	-48.1	-47.3	-59.7

[a]Structures optimized and vibrational frequencies calculated at B3LYP/6-31(d)(C,H)/6-31+G(d)(N,O)/ LANL2DZ(Re) with CPCM implicit solvent model for acetone.

[b]ΔE (SMD) is the electronic energy computed with the SMD implicit solvent model

[c]ΔE (CPCM) and ΔG (CPCM) are the electronic energy and thermal free energy, respectively, computed with the CPCM implicit solvent model

[d]ΔG (SMD corr.) is the thermal free energy evaluated as recommended in ref. S8 with CPCM solvent model.

[e]ΔG (vib. only) is the same as ΔG (SMD corr.) but considering only vibrational thermal energy (i.e. neglecting translational and rotational contributions)

A Hammett equation has been applied to complexes **1a-1d**. The k_o is the reaction rate of nonsubstituted bipyridine (**1e**, R = H). σ values of *para*-effect adopted from Hammett, L.P. were applied to make the plot as shown in Figure S4. A linear plot with R^2 = 0.972 and reaction constant ρ= 1.3716 were obtained.

Complex	σ_p	**Log k/k$_o$**
-OMe, **1c**	-0.170	-0.243
-Me, **1b**	-0.268	-0.301
-H, **1a**	0.000	0.000
-Cl, **1d**	0.227	0.301
-Br, **1e**	0.232	0.398

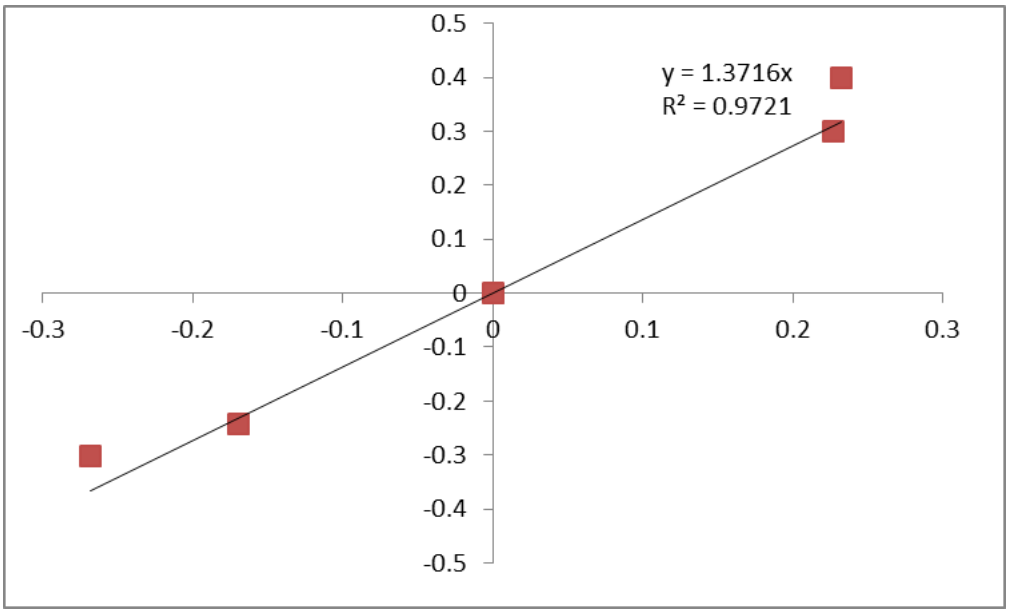

Figure S4. Plot of Hammett equation with *para*-effect σ value.

References:

S1. Worl, L. A.; Duesing, R.; Chen, P.; Ciana, L. D.; Meyer, T. J. Photophysical Properties of Polypyridyl Carbonyl Complexes of Rhenium(1). *J. Chem. Soc. Dalton Tran.s* **1991**, 848–858.

S2. a.Sullivan, B. P.; Meyer, T. J. Photoinduced irreversible insertion of CO2 into a Metal-Hydride bond. *J. Chem. Soc., Chem. Commun.* **1984**, 1244–1245. Sullivan, B. P.; Meyer, T. J. Kinetics and Mechanism of CO, Insertlon Into a Metal-Hydride Bond. A Large Solvent Effect and an Inverse Kinetic Isotope Effect *Organometallics* **1986**, 5, 1500–1502.

S3. Gibson, D. H.; Yin, X. Synthesis and Reactions of *Fac*-Re(Dmbpy)$(CO)_3$X (Dmbpy = 4,4'-Dimethyl-2,2'-Bipyridyl; X = COOH, COOMe, H, OH, and OCHO). *J. Am. Chem. Soc.* **1998**, *120*, 11200–11201.

S4. Gaussian 09, Revision D.01, M. J. Frisch, G. W. Trucks, H. B. Schlegel, G. E. Scuseria, M. A. Robb, J. R. Cheeseman, G. Scalmani, V. Barone, G. A. Petersson, H. Nakatsuji, X. Li, M. Caricato, A. Marenich, J. Bloino, B. G. Janesko, R. Gomperts, B. Mennucci, H. P. Hratchian, J. V. Ortiz, A. F. Izmaylov, J. L. Sonnenberg, D. Williams-Young, F. Ding, F. Lipparini, F. Egidi, J. Goings, B. Peng, A. Petrone, T. Henderson, D. Ranasinghe, V. G. Zakrzewski, J. Gao, N. Rega, G. Zheng, W. Liang, M. Hada, M. Ehara, K. Toyota, R. Fukuda, J. Hasegawa, M. Ishida, T. Nakajima, Y. Honda, O. Kitao, H. Nakai, T. Vreven, K. Throssell, J. A. Montgomery, Jr., J. E. Peralta, F. Ogliaro, M. Bearpark, J. J. Heyd, E. Brothers, K. N. Kudin, V. N. Staroverov, T. Keith, R. Kobayashi, J. Normand, K. Raghavachari, A. Rendell, J. C. Burant, S. S. Iyengar, J. Tomasi, M. Cossi, J. M. Millam, M. Klene, C. Adamo, R. Cammi, J. W. Ochterski, R. L. Martin, K. Morokuma, O. Farkas, J. B. Foresman, and D. J. Fox, Gaussian, Inc., Wallingford CT, 2016.

S5. Fujita, E.; Muckerman, J. T. Why Is Re−Re Bond Formation/Cleavage in $[Re(Bpy)(CO)_3]_2$ Different from That in $[Re(CO)_5]_2$ Experimental and Theoretical Studies on the Dimers and Fragments. *Inorg. Chem.* **2004**, *43*, 7636–7647. https://doi.org/10.1021/ic048910v.

S6. A. S. Grimme, J. Antony, S. Ehrlich and H. Krieg, "A consistent and accurate ab initio parameterization of density functional dispersion correction (DFT-D) for the 94 elements H-Pu," *J. Chem. Phys.*, **2010**, *132,* 154104. DOI: 10.1063/1.3382344 b. M. Cossi, N. Rega, G. Scalmani, and V. Barone, "Energies, structures, and electronic properties of molecules in solution with the C-PCM solvation model," *J. Comp. Chem.*, **2003**, 24, 669-81. DOI: 10.1002/jcc.10189

S7. A. V. Marenich, C. J. Cramer, and D. G. Truhlar, "Universal solvation model based on solute electron density and a continuum model of the solvent defined by the bulk dielectric constant and atomic surface tensions," *J. Phys. Chem. B*, **2009**, 113, 6378-96. DOI: 10.1021/jp810292n

S8. Foresman, James B, Frisch Æleen: Exploring Chemistry with Electronic Structure Methods, 3rd Ed., Gaussian, Inc, Walingford CT, USA, 2015.